

## Asymmetry and Electronegativity in the Electron Capture Activation of the Se—Se Bond: $\sigma^*(\text{Se—Se})$ vs $\sigma^*(\text{Se—X})$

José A. Gámez and Manuel Yáñez\*

Departamento de Química, Módulo 13, Universidad Autónoma de Madrid, Campus de Excelencia UAM-CSIC, Cantoblanco, E-28049 Madrid, Spain

Received June 18, 2010

**Abstract:** The effects of electron capture on the structure of XSeSeX' diselenide derivatives in which the substituents attached to the selenium atoms have different electronegativities have been investigated at different levels of theory, namely, DFT, MP2, CCSD, G2, and CASSCF/CASPT2. An analysis of the bonding changes upon electron attachment shows that when the diselenides bear low-electronegativity substituents, the Se—Se bond becomes activated upon electron capture, as previous studies have shown. However, this is no longer the case for very electronegative substituents, where this bond remains practically unaltered and is the Se—X bond the one which becomes strongly activated through a preferential population of the  $\sigma^*(\text{Se—X})$  antibonding orbital rather than the  $\sigma^*(\text{Se—Se})$  one. When this is the case, several anionic species are also encountered, namely, *stretched*, *bent*, and *book* structures. The present findings are similar to those obtained for a series of analogous disulfide compounds, which points out that these results are not unique and could be extrapolated to a wider range of compounds than the ones covered here. The Se—Se (Se—X) linkage in CH<sub>3</sub>SeSeOH, CH<sub>3</sub>SeSeF, FSeSeOH, and FSeSeF bears some of the characteristics of the so-called charge-shift bonds, with a clear charge fluctuation between both selenium atoms. This is more evident in their anions where the bonding reflects the important contribution of the ionic resonant forms Se—Se<sup>—</sup> ↔ Se—Se<sup>+</sup> vs the covalent component Se<sup>.</sup>:Se. This resonance changes with the nature of the substituents but also depends on the asymmetry of the substitution.

### Introduction

The abundance of selenium in the Earth's crust is about 4 times lower than that of sulfur, which is reflected in the amount in which these elements are present in biological systems. However, except for tellurium, chalcogens are fundamental constituents of functional groups of amino acids and are important contributors to the chemistry and structure of peptides and proteins. Selenium is a trace element present in milligram amounts in the human body. In spite of its low abundance, selenium has been identified as an essential trace element for bacteria, birds, and mammals.<sup>1</sup> It is present in proteins in the form of selenocysteine and selenomethionine and has been observed in various oxidation states such as the reactive selenol, selenic acid, selenoxid, and selenylsulfide and the recently discovered diselenide bond.<sup>2</sup> Many seleno-

proteins have been identified in many living beings<sup>3,4</sup> and 25 in humans.<sup>5</sup> These proteins act as antioxidant agents, eliminating peroxides from the organism, and are also involved in cancer prevention and inflammation protection.<sup>6–8</sup>

Sulfur and selenium have many common characteristics. Actually, in living organisms, selenium usually accompanies or substitutes sulfur thanks to its comparable physicochemical properties. Indeed, the mutation of cysteine (Cys) to selenocysteine (Sec) has been studied in a large variety of proteins.<sup>9–19</sup> In all cases, the selenium analogues folded correctly, and the NMR structural analysis and CD spectroscopy confirm that the protein structure suffers from little distortion after substitution by selenium. Importantly, full biological activity was observed in all cases, confirming that the substitution of Cys by Sec is quite conservative. Nevertheless, this substitution has significant advantages over a substitution with other chemical moieties, which can import

\* Corresponding author e-mail: manuel.yanez@uam.es.

structural distortions which may compromise bioactivity and selectivity.<sup>20–23</sup> For example, selenoproteins with known functions are oxyreductases containing catalytic redox-active Sec,<sup>24</sup> whereas their Cys mutants are typically 100–1000 times less active.<sup>25</sup>

Among the huge family of selenium-containing compounds, diselenides are of special interest. They are used in organic synthesis as precursors of organic selenium derivatives<sup>26–28</sup> and as therapeutic drugs,<sup>29,30</sup> and as mentioned above, they can form diselenide bridges in proteins<sup>2</sup> analogous to the disulfide linkages in Cys-containing peptides. Diselenides are well-known for their high antioxidant activity,<sup>31–33</sup> which is actually higher than that of disulfides. In this respect, the work of Pearson and Boyd is noteworthy,<sup>34</sup> where they found, by means of DFT calculations, that the reduction of hydrogen peroxide by ebselene diselenide is favored with respect to its disulfur analogue due to lower energy barriers for the reactions of the former. However, the little literature available on this topic prevents a general picture of the main reasons behind this behavior. Also, in contrast with disulfides, where this process has been studied much more extensively,<sup>35–39</sup> little attention has been paid to the change of the electronic structure of diselenides in the very first stage of the reduction: the electron attachment process. Previous studies<sup>40,41</sup> indicate that electron attachment to dimethyldiselenide yields mainly the fragmentation of the Se—Se bond since the extra electron is accommodated in the  $\sigma^*(\text{Se—Se})$  antibonding orbital, as it occurred for disulfides. However, to the best of our knowledge, there is a complete lack of data concerning asymmetric diselenides or diselenides bearing substituents with different electronegativities. We have recently shown for disulfides bearing highly electronegative substituents<sup>42</sup> that the electron capture process leads to dissociations different from that of the S—S bond, as had been previously assumed. The aim of this paper is to investigate the changes in the electronic structure of asymmetric diselenides, and their consequences, upon electron capture. The  $\text{CH}_3\text{SeSeX}$  ( $X = \text{NH}_2, \text{OH}, \text{and F}$ ) set of molecules has been chosen as a suitable model ensemble, which include substituents of increasing electronegativity that can be compared with  $\text{HSeSeH}$  and  $\text{CH}_3\text{SeSeCH}_3$  to determine the influence of the asymmetry in the electron-attachment process.

## Computational Methods

Density functional theory (DFT) is quite popular in the quantum chemistry community due to its high accuracy at a low computational price. However, approximate functionals suffer from the self-interaction error (an unbalanced description of the Coulomb and exchange terms), which becomes especially important for odd-electron systems,<sup>43–45</sup> as is the case in this study. More recently, this problem has been renamed delocalization error,<sup>46</sup> present when, due to delocalization, atomic centers bear fractional charges, causing approximate functionals to underestimate the energy of such systems. As a result, DFT methods predict too large electron affinities or bond lengths, when an electron is added to a closed-shell molecule to form an open-shell anion,<sup>47–49</sup> as in the present study. Additionally, DFT overestimates the

bond length and the binding energy of two-center–three-electron linkages ( $2c-3e$ ),<sup>50</sup> which casts serious doubts on the reliability of DFT for this kind of system. However, since HF overestimates the energy of such charge-delocalized systems, the use of the BH&H functional proposed by Becke<sup>51</sup> including 50% exact exchange seems a good compromise. Actually, this exchange functional combined with the LYP correlation functional<sup>52</sup> has shown good performance for the kinds of systems considered here.<sup>50</sup> We have also used the MP2 method because it usually yields good results for the types of systems here investigated. However, it should be taken into account that sometimes the  $2c-3e$  bonds are not properly described at the HF level, in which case the MP2 results would be questionable.<sup>53</sup> Hence, CCSD(T), which includes a large amount of correlation energy and will give results close to the experimental value, will be used to assess the other methods. In addition to that, G2 estimates, which are known to provide an accurate description of these systems,<sup>54,55</sup> have also been included for the computation of the electron affinities.

The 6-31++G(d,p) (BS1) basis set will be used for geometry optimizations, since it provides enough flexibility to describe the bonding situations we deal with. Diffuse functions are necessary to describe the extra electron placed far from the nuclei in the anions. To ensure that the optimized geometries were true minima, the Hessian matrix has been evaluated. Although the basis set BS1 is flexible enough for geometry optimizations, final energies will be obtained with single-point calculations with a larger aug-cc-pVTZ basis set (BS2). The geometry optimizations and Hessian evaluations with BS1 and single-point DFT calculations with BS2 have been performed with the Gaussian 03 suite of programs,<sup>56</sup> while the single point calculations with BS2 at the MP2 and CCSD(T) levels were carried out with the MOLPRO 2009.01 package.<sup>57</sup>

Since this study involves radicals, in some cases the nature of the wave function and the reliability of the results had to be checked to determine the single- or multiconfigurational character of the states. Multireference methods have been included in this study, in particular, the CASSCF/CASPT2 approach. Geometries were optimized at the CASSCF level with the atomic natural orbital (ANO) basis set described by Pierloot et al.<sup>58</sup> contracted to  $\text{Se}[5s4p3d]/\text{C,N,O,F}[3s2p1d]/\text{H}[2s1p]$  (BS3). With these geometries, high-level energies were obtained with the second-order perturbation multireference CASPT2 method using the same BS2 as for the other methods. The active space was formed by distributing 10 electrons (11 in the case of anions) in eight orbitals (nine for the anions), which showed good results in a similar study involving disulfides.<sup>42</sup> The multireference calculations were performed with the MOLCAS 7.2 package of programs.<sup>59</sup>

To fully understand the nature of the bonds of the species under study, an atoms in molecules (AIM) analysis<sup>60</sup> has been performed. For this purpose, the electron and energy densities at the different bond critical points (BCPs) have been evaluated to gain some insight into the different changes produced upon electron attachment. This analysis has been carried out with the DGrid 4.5 program.<sup>61</sup> Further information about the electronic rearrangement of the diselenide

**Table 1.** Main Internal Coordinates of the Neutral (Radical–Anionic) HSeSeH, CH<sub>3</sub>SeSeCH<sub>3</sub>, and CH<sub>3</sub>SeSeNH<sub>2</sub> Species Calculated with Several Methods and the 6-31++G(d,p) (BS3 for CASSCF) Basis Set<sup>a</sup>

Compound					
	HSeSeH				
d(Se–Se)	BH&HLYP (2.998)	MP2 (2.948)	CCSD (2.985)	CASSCF (3.080)	Literature <sup>55</sup> 2.355, 2.370
d(Se–H)	1.472 (1.472)	1.484 (1.483)	1.492 (1.493)	1.486 (1.489)	1.463, 1.476
∠SeSeH	97.0 (88.9)	96.6 (89.1)	96.5 (89.1)	95.5 (86.1)	
HSeSeH	91.6 (90.1)	90.3 (92.8)	90.3 (92.5)	90.0 (93.0)	90.67, 90.5
Compound					
	CH <sub>3</sub> SeSeCH <sub>3</sub>				
d(Se–Se)	BH&HLYP (2.980)	MP2 (2.929)	CCSD (2.965)	CASSCF (3.069)	Exp. <sup>66</sup> 2.306, 2.326
d(Se–X)	1.949 (1.954)	1.966 (1.958)	1.965 (1.973)	1.999 (2.013)	1.954, 1.945
∠SeSeX	100.2 (83.3)	99.0 (85.9)	99.1 (86.3)	99.8 (90.2)	99.8, 98.9
CSeSeX	87.7 (86.9)	86.1 (85.5)	86.5 (85.7)	87.7 (88.1)	85.2, 87.5
Compound					
	CH <sub>3</sub> SeSeNH <sub>2</sub>				
d(Se–Se)	BH&HLYP (3.011)	MP2 (2.957)	CCSD (2.996)	SS-CASSCF (3.202)	SA-CASSCF (3.055)
d(Se–X)	1.826 (1.881)	1.847 (1.905)	1.889 (1.910)	1.859 (1.913)	1.859 (1.954)
∠SeSeX	106.6 (88.3)	106.9 (90.2)	106.2 (90.0)	106.8 (90.4)	106.8 (94.6)
CSeSeX	89.4 (89.9)	87.3 (82.9)	87.6 (85.1)	88.4 (89.9)	88.4 (90.6)

<sup>a</sup> Bond lengths are given in Å and angles in degrees.

derivatives in these processes was achieved by means of the Becke and Edgecombe electron localization function<sup>62</sup> (ELF) approach.<sup>63</sup> ELF is a function which measures the probability of finding an electron pair at a given region of the space, so it becomes large in regions where electron pairs are localized, either as bonding or lone pairs. By means of an appropriate Lorentzian transform, ELF can be confined in the [0,1] interval. In this way, the molecular space can be divided in polysynaptic (generally disynaptic) basins, with the participation of two (or more) atomic valence shells and monosynaptic ones, which correspond to core electrons or lone pairs.<sup>64</sup> ELF grids and basin integrations have been evaluated with the TopMod package.<sup>65</sup>

## Geometrical Changes upon Electron Attachment

Tables 1 and 2 summarize the geometric changes of HSeSeH and CH<sub>3</sub>SeSeX (X = CH<sub>3</sub>, NH<sub>2</sub>, OH, F) triggered upon electron capture. To the best of our knowledge, experimental

information is only available for the neutral dimethyldiselenide,<sup>66</sup> whereas for neutral HSeSeH just theoretical estimates have been previously reported.<sup>55</sup> The values calculated for these compounds agree well with those found in the literature, which confirms the reliability of the approach used.

For the compounds in Table 1 (HSeSeH, CH<sub>3</sub>SeSeCH<sub>3</sub>, and CH<sub>3</sub>SeSeNH<sub>2</sub>), the main geometrical deformation observed after electron attachment is the lengthening of the Se–Se bond by ca. 0.6 Å, while the other geometrical parameters remain practically unperturbed. All the methods employed provide rather similar geometries for the radical anions, although MP2 underestimates the lengthening of the Se–Se bond relative to the CCSD and BH&HLYP values. This was explained by Bräida and Hiberty<sup>53</sup> on the basis of a dissimilar charge distribution along the 2c–3e bond (Se–Se) at the UHF and UMP2 levels, which has not been found in this case (see Table S2 of the Supporting Information). This discrepancy could

**Table 2.** Main Internal Coordinates of the Neutral and Anionic Species of  $\text{CH}_3\text{SeSeOH}$  and  $\text{CH}_3\text{SeSeF}$  Calculated with Several Methods and the 6-31++G(d,p) (BS3 for CASSCF) Basis Set<sup>a</sup>

Isomer	$\text{CH}_3\text{SeSeOH}$					$\text{CH}_3\text{SeSeF}$					
	BH&HLYP	MP2	CCSD	SS-CASSCF	SA-CASSCF	BH&HLYP	MP2	CCSD	SS-CASSCF	SA-CASSCF	
d(Se-Se)	Neutral	2.286	2.295	2.310	2.316	2.703	2.256	2.262	2.280	2.326	2.381
	Stretched	2.547	2.529	2.557	2.806		2.428	2.428	2.443	2.449	
	Bent	2.325	2.333	2.350	2.347		2.304	2.314	2.329	2.364	
	Book	2.938	2.894	2.929	3.023						
d(Se-X)	Neutral	1.799	1.833	1.830	1.852	2.025	1.771	1.803	1.793	1.798	2.540
	Stretched	1.987	2.032	2.016	1.941		2.029	2.050	2.065	2.165	
	Bent	2.404	2.235	2.363	2.431		2.278	2.270	2.286	2.568	
	Book	1.847	1.884	1.883	1.893						
$\angle\text{SeSeX}$	Neutral	103.1	102.7	102.0	103.3	145.8	101.6	101.7	101.0	100.8	86.8
	Stretched	151.6	160.2	153.0	151.1		159.9	160.1	161.3	162.7	
	Bent	92.0	91.0	90.6	98.7		88.4	88.2	86.5	85.6	
	Book	82.1	81.3	81.8	85.7						
CSeSeX	Neutral	82.4	81.1	81.0	82.1	82.6	85.7	85.8	85.7	84.8	49.4
	Stretched	80.7	79.3	79.8	82.9		85.5	83.3	83.6	89.0	
	Bent	50.8	48.3	51.0	53.3		54.8	56.3	55.3	48.5	
	Book	85.2	82.0	81.6	82.5						

<sup>a</sup> Bond lengths are given in Å and angles in degrees.

be better attributed to the large electronic correlation needed to describe the outer electrons of Se not completely recovered by MP2.

The good performance of the BH&HLYP functional is remarkable, giving results quite close to the highly correlated CCSD estimates. CASSCF presents larger deviations than MP2 due to the missing dynamic correlation. Regarding these estimates for  $\text{CH}_3\text{SeSeNH}_2$ , two values are presented. The first ones, state specific CASSCF (SS-CASSCF), were obtained by optimizing the ground state wave function, without considering any other state. However, this resulted in a somewhat large overestimation of the Se–Se lengthening upon electron capture. An optimization of the lowest root of a state average CASSCF (SA-CASSCF) comprising the six lowest states shows better results, probably due to the fact that in the SS-CASSCF wave function the  $\sigma^*(\text{Se–Se})$  had an unphysical high contribution in the total wave function, corrected with the averaging procedure.

Regarding  $\text{CH}_3\text{SeSeOH}$  and  $\text{CH}_3\text{SeSeF}$  (see Table 2), the first remarkable feature is that the electron capture process leads to more than one stable radical anion: two for the fluorine derivative and three for  $\text{CH}_3\text{SeSeOH}$ , as it has been previously found for the disulfide analogues.<sup>42</sup> The *stretched* isomers are characterized by a moderate elongation of about 0.2 Å for the Se–Se and Se–X bonds and by a substantial opening of the SeSeX angle, whereas the *bent* anions show a significant elongation (ca. 0.5 Å) of the Se–X bond and a decrease of the CSesex dihedral angle. The *book* isomer, which is unique for  $\text{CH}_3\text{SeSeOH}$ , has a book-like conformation similar to that of the neutral species, but with a longer (ca. 0.6 Å) Se–Se bond. Again, the three methods agree well in their predictions, especially BH&HLYP and CCSD. The deviations of SS-CASSCF in the *stretched* anion of

**Table 3.** Relative Stability in Terms of  $\Delta H$  ( $\Delta G$  in parentheses) at 298 K of the Different Anions Present for the  $\text{CH}_3\text{SeSeOH}$  and  $\text{CH}_3\text{SeSeF}$  Structures Calculated with the aug-cc-pVTZ Basis Set<sup>a</sup>

	BH&HLYP	MP2	CCSD(T)	CASPT2	G2
stretched $\text{CH}_3\text{SeSeOH}$	0 (0)	0 (0)	0 (0)	0 (0)	0 (0)
bent $\text{CH}_3\text{SeSeOH}$	32 (36)	43 (46)	36 (40)	17 (20)	36 (44)
book $\text{CH}_3\text{SeSeOH}$	9 (10)	16 (17)	11 (12)	14 (15)	18 (20)
stretched $\text{CH}_3\text{SeSeF}$	0 (0)	0 (0)	0 (0)	0 (0)	0 (0)
bent $\text{CH}_3\text{SeSeF}$	27 (29)	29 (31)	29 (31)	34 (37)	24 (30)

<sup>a</sup> Values in kJ mol<sup>-1</sup>.

$\text{CH}_3\text{SeSeOH}$  are corrected with the averaging procedure but not for the *bent* isomer of  $\text{CH}_3\text{SeSeF}$ . Among this collection of anionic derivatives, the most stable species among this series of isomers correspond to the *stretched* one (Table 3), the *book* one being intermediate between the *stretched* and the *bent* structures. However, the energy gap between them suggests that upon electron attachment the only product would be the *stretched* anion. This is in contrast to what was found for disulfides, where the small energy gaps between the different anionic structures predicted that a mixture of them should be obtained.

All the anionic structures presented here correspond to minima of the potential energy surface (PES). However, to ensure that they are really stable anions, the eigenvalue of the HF SOMO has been checked, being negative in all cases (see Table S3 of the Supporting Information). Another assessment of the stability of these anions, experimentally

**Table 4.** Adiabatic Electron Affinities ( $\text{EA}_{\text{adiab}}$ ) in terms of  $\Delta H$  ( $\Delta G$  in parentheses) at 298K calculated with the aug-cc-pVTZ Basis Set<sup>a</sup>

	BH&HLYP	MP2	CCSD(T)	CASPT2	G2
HSeSeH	107 (115)	95 (103)	102 (110)	89 (96)	94 (101)
CH <sub>3</sub> SeSeCH <sub>3</sub>	53 (59)	45 (52)	53 (60)	44 (50)	44 (55)
CH <sub>3</sub> SeSeNH <sub>2</sub>	48 (58)	40 (50)	49 (59)	46 (53)	41 (55)
CH <sub>3</sub> SeSeOH	72 (79)	75 (79)	73 (79)	78 (85)	72 (83)
CH <sub>3</sub> SeSeF	124 (132)	120 (128)	124 (132)	130 (138)	121 (130)

<sup>a</sup> Values in kJ mol<sup>-1</sup>.

measurable, is the adiabatic electron affinity ( $\text{EA}_{\text{adiab}}$ ), which has been found positive for all of the species (see Table 4).

Although all values are similar, the very good agreement between the BH&HLYP and the CCSD(T) results is worth noting, while the MP2 and CASPT2 values bear better resemblance to the G2 ones. To the best of our knowledge, only the vertical electron affinity ( $\text{EA}_v$ ) of CH<sub>3</sub>SeSeCH<sub>3</sub> has been experimentally measured by Modelli et al.,<sup>41</sup> which obtained a value of 0.27 eV, in clear contrast with our theoretical estimates: 0.55, 0.55, 0.49, and 0.57 eV for BH&HLYP, MP2, CCSD(T), and CASPT2 respectively. However, the value reported by the same authors for CH<sub>3</sub>SSCH<sub>3</sub> (1.04 eV) is much smaller than the value of 1.75 eV given by Carles et al.,<sup>67</sup> which is nicely reproduced by our theoretical approaches (1.81 and 1.69 eV for MP2 and CASPT2, respectively), suggesting that the values of Modelli and co-workers could be underestimated. Interestingly, when these EA values are compared with those of the disulfide analogues,<sup>42</sup> one finds that the EA is higher for diselenides than for disulfides, probably due to the fact that for the former the extra electron is accommodated in a more diffuse orbital, leading to a lower interelectronic repulsion. This higher EA could also be behind the stronger antioxidant activity of diselenides compared to disulfides.

## The Nature of the Anions

To better understand the geometrical changes triggered by the electron capture process, it is necessary to gain some insight into the modifications that this extra electron induces in the electronic structure of the system. As indicated above, those anions presenting only one stable isomer show a significant lengthening of the Se—Se bond, whereas other geometrical parameters remain practically unperturbed.

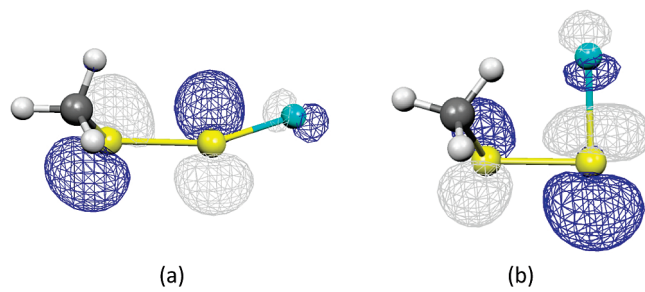


**Figure 2.** SOMOs of the (a) stretched and (b) bent anions of CH<sub>3</sub>SeSeF. Selenium atoms are in yellow, carbon ones in gray, fluorine in cyan, and hydrogen in white.

Previous studies on diselenides show the lability of the Se—Se linkage upon electron attachment, which is coherent with this bond elongation. Actually, the peak of least energy of the electron-transmission spectrum of CH<sub>3</sub>SeSeCH<sub>3</sub> has been attributed to the occupancy by the extra electron of the  $\sigma^*(\text{Se—Se})$  antibonding orbital,<sup>41</sup> which is confirmed by our theoretical calculations as shown in Figure 1.

However, when the electron attachment process leads to more than one stable anion, the bonding situation is very different. As the substituent becomes more and more electronegative, the contribution of its orbitals to the single-occupied molecular orbital (SOMO) increases (see Figure 2 for the particular case of the fluorine derivative), in an attempt to displace the electronic density associated with the extra electron toward the more electronegative substituent.

Hence, in both the *stretched* and the *bent* isomers of CH<sub>3</sub>SeSeF, the SOMO arises from a linear combination of the  $\sigma^*(\text{Se—F})$  and  $\pi^*(\text{Se—Se})$  antibonding orbitals. This explains the moderate elongation of the Se—Se linkage, since the  $\sigma$  component of the bond is not affected in any case, and the increase in the Se—F distance, since the SOMO always has a significant  $\sigma^*(\text{Se—F})$  antibonding character. The larger contribution of the  $\sigma^*(\text{Se—F})$  MO in the SOMO would explain the longer Se—F bond of the *bent* anion relative to the *stretched* isomer. This is not easily seen in Figure 2, but an examination of the spin density (see Table S4 of the Supporting Information) shows that for the *bent* isomer the density is accumulated preferentially at the F atom and the Se atom to which it is attached (0.21 and 0.76, respectively), whereas for the *stretched* isomer, the spin density at the F atom is very small (0.07).

The CH<sub>3</sub>SeSeOH can be viewed as an intermediate situation between the compounds in Table 1 and CH<sub>3</sub>SeSeF. Indeed, an anionic structure (*book* anion) can be found whose SOMO is the  $\sigma^*(\text{Se—Se})$  antibonding MO (Figure 3), like

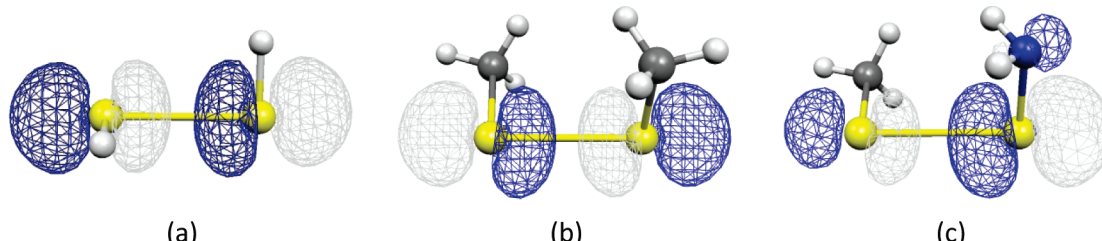


**Figure 1.** Single occupied molecular orbital (SOMO) for the radical-anionic derivatives of (a) HSeSeH, (b) CH<sub>3</sub>SeSeCH<sub>3</sub>, and (c) CH<sub>3</sub>SeSeNH<sub>2</sub>. Selenium atoms are in yellow, carbon ones in gray, nitrogen in blue, and hydrogen in white.

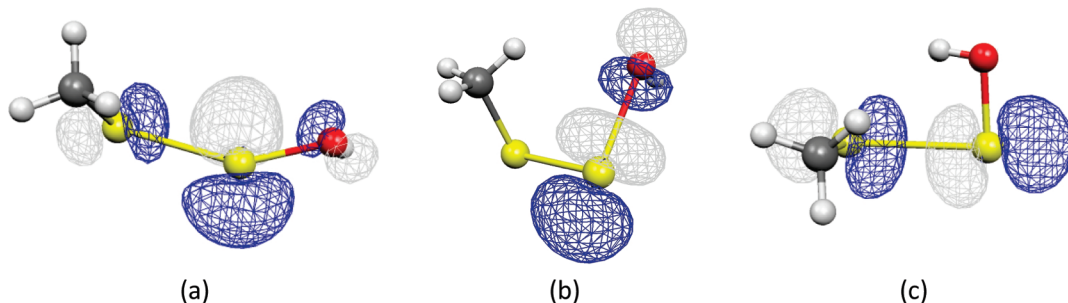


**Figure 3.** SOMOs of the (a) stretched, (b) bent, and (c) book anions of  $\text{CH}_3\text{SeSeOH}$ . Selenium atoms are in yellow, carbon ones in gray, oxygen in red, and hydrogen in white.

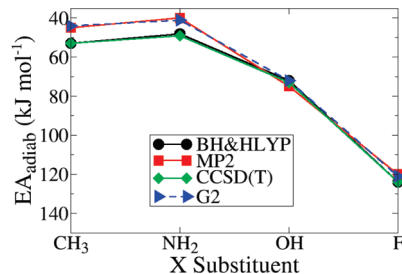


**Figure 4.** Adiabatic EA as a function of X for the  $\text{CH}_3\text{SeSeX}$  series of compounds. It should be noted that the energy scale is inverted from the normal order.

in  $\text{CH}_3\text{SeSeNH}_2$ , and another one (*bent* anion) which has the  $\sigma^*(\text{Se}-\text{O})$  antibonding orbital as SOMO, similar to what has been found for  $\text{CH}_3\text{SeSeF}$ . Actually, there exists a third anion (*stretched* anion) whose SOMO is intermediate between the previous two orbitals, presenting two nodes: one at the Se—Se bond and the other at the Se—O one. The nature of the SOMOs just discussed offers useful clues to rationalize why the *book* isomer presents quite a long Se—Se bond and why for the *bent* isomer just the Se—O linkage becomes activated, whereas for the *stretched* derivative both distances partially increase.

Similarly to what has been previously reported for disulfide derivatives,<sup>35,42</sup> when increasing the electronegativity of the substituent, the SOMO loses its  $\sigma^*(\text{Se}-\text{Se})$  nature and gains

some  $\sigma^*(\text{Se}-\text{X})$  character. This permits rationalization of the unexpected variation of the  $\text{EA}_{\text{adiab}}$  in the  $\text{CH}_3\text{SeSeX}$  series. As shown in Figure 4, while the electronegativity of X increases as  $\text{CH}_3 < \text{NH}_2 < \text{OH} < \text{F}$ , the same trend is not observed for the  $\text{EA}_{\text{adiab}}$  values, since surprisingly, the electron affinity of  $\text{CH}_3\text{SeSeNH}_2$  is lower than that of  $\text{CH}_3\text{SeSeCH}_3$ . When the electronegativity of the substituent X increases, the  $\sigma^*(\text{Se}-\text{X})$  MO becomes stabilized at the price of destabilizing the  $\sigma^*(\text{Se}-\text{Se})$ , explaining the aforementioned variation of the electron affinity between  $\text{CH}_3\text{SeSeCH}_3$  and  $\text{CH}_3\text{SeSeNH}_2$ . Once the  $\sigma^*(\text{Se}-\text{X})$  MO is lower in energy than the  $\sigma^*(\text{Se}-\text{Se})$  MO, the increase of the electronegativity of X just stabilizes it further, which explains why the  $\text{EA}_{\text{adiab}}$  of  $\text{CH}_3\text{SeSeF}$  is larger than that of  $\text{CH}_3\text{SeSeOH}$ .

### The Nature of the Bonding

**The Se—Se Bond.** As expected, the aforementioned structural changes upon electron capture just reflect concomitant changes in the electronic structure. For  $\text{X} = \text{H}$ ,  $\text{CH}_3$ , or  $\text{NH}_2$ , a significant decrease of the electron density at the Se—Se BCP is observed (Table 5). This fact, together with the positive value of  $\nabla^2\rho$  and the near-zero energy density at this point, seems to indicate that the Se—Se interaction comes mainly from dispersion, which is also supported by the fact that the ELF does not present a disynaptic basin  $V(\text{Se},\text{Se})$  for these compounds (Figure 5).

**Table 5.** Electronic Density,  $\rho$  (in  $\text{e a}_0^{-3}$ ),  $\nabla^2\rho$  (in  $\text{e a}_0^{-5}$ ), and Energy Density,  $H$  (in  $\text{E}_h \text{a}_0^{-3}$ ), Evaluated at the BCP of the Se—Se and Se—X Bonds for the  $\text{CH}_3\text{SeSeX}$  Set of Molecules Calculated at the BH&HLYP/6-31++G(d,p) Level

		Se—Se			Se—X		
		$\rho$	$\nabla^2\rho$	$H$	$\rho$	$\nabla^2\rho$	$H$
$\text{HSeSeH}$	neutral	0.1070	-0.0764	-0.0529	0.1717	-0.2015	-0.1363
	anion	0.0307	0.0576	-0.0004	0.1649	-0.1497	-0.1273
$\text{CH}_3\text{SeSeCH}_3$	neutral	0.1105	-0.0820	-0.0564	0.1489	-0.1567	-0.0982
	anion	0.0321	0.0578	-0.0008	0.1416	-0.1072	-0.0907
$\text{CH}_3\text{SeSeNH}_2$	neutral	0.1098	-0.0753	-0.0556	0.1606	0.1435	-0.1120
	anion	0.0312	0.0582	-0.0006	0.1439	0.1199	-0.0912
$\text{CH}_3\text{SeSeOH}$	neutral	0.1161	-0.0894	-0.0621	0.1497	-0.1649	-0.0987
	stretched	0.0649	0.0482	-0.0181	0.0942	0.2089	-0.0300
	bent	0.1014	-0.0549	-0.0474	0.0509	0.1585	-0.0020
$\text{CH}_3\text{SeSeF}$	book	0.0354	0.0613	-0.0018	0.1279	0.2122	-0.0661
	neutral	0.1215	-0.0980	-0.0680	0.1394	0.4467	-0.0708
	stretched	0.0843	0.0263	-0.0335	0.0820	0.2362	-0.0204
$\text{OHSeSeF}$	bent	0.1100	-0.0714	-0.0559	0.0552	0.1814	-0.0048
	neutral	0.1235	-0.0978	-0.0701	0.1364	0.4021	-0.0694
$\text{FSeSeF}$	anion	0.0966	0.0229	-0.0449	0.0755	0.2140	-0.0167
	neutral	0.1341	-0.1165	-0.0826	0.1432	0.4585	-0.0742
	anion	0.1060	-0.0002	-0.0535	0.0953	0.2469	-0.0313

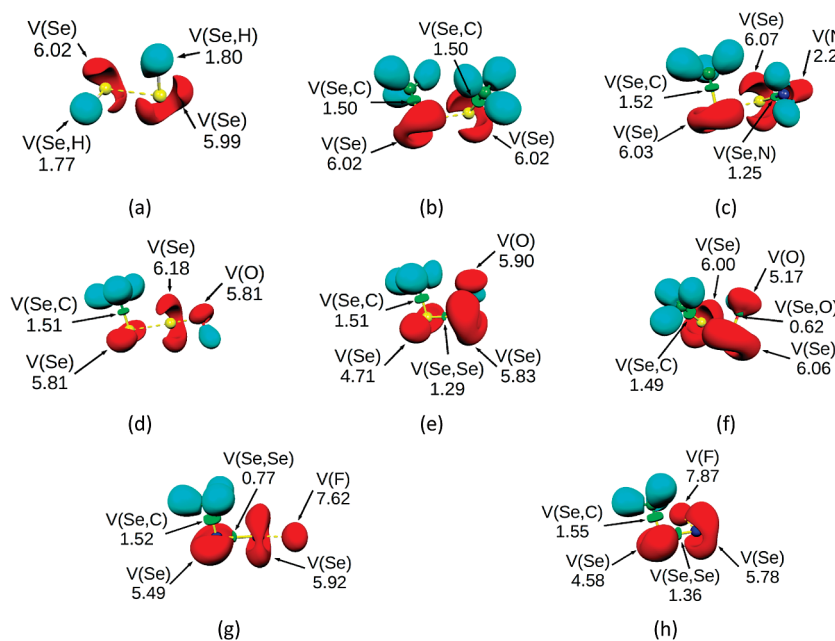


**Figure 5.** ELF localization domains within the isosurface ELF = 0.8 for the anionic derivatives of (a) HSeSeH, (b) CH<sub>3</sub>SeSeCH<sub>3</sub>, (c) CH<sub>3</sub>SeSeNH<sub>2</sub>, (d) *stretched*, (e) *bent*, and (f) *book* isomers of CH<sub>3</sub>SeSeOH and (g) *stretched* and (h) *bent* anions of CH<sub>3</sub>SeSeF molecules. Blue lobes correspond to basins involving H atoms (protonated basins), green lobes to disynaptic basins between two bonding atoms, and red ones refer to monosynaptic lone-pair basins. The population of the different basins is given in e.

These topological features are typically encountered in 2c–3e bonds. However, these linkages usually present dissociation energies much larger than those expected from dispersion because a charge fluctuation between the atoms,<sup>68–71</sup> due to the similar distribution of the unpaired electron between them, takes place. In fact, an exponential decrease of the dissociation energy of cationic (anionic) 2c–3e bonds with the relative IP (EA) of the constituent fragments was found both by experimental<sup>72</sup> and theoretical<sup>70</sup> means, which indicates that 2c–3e bonds are stronger the more evenly distributed between the fragments the unpaired electron is.

Obviously for symmetric systems like HSeSeH and CH<sub>3</sub>SeSeCH<sub>3</sub>, both fragments have the same EA value and hence present strong bonds. Conversely, for CH<sub>3</sub>SeSeNH<sub>2</sub>, where the value of  $\Delta$ EA increases, a bond weakening is observed (see Table 6). Since an important component of 2c–3e bonds is a charge fluctuation between the bonding atoms, it would be useful to estimate the extent of such delocalization. This is possible through the delocalization indexes<sup>73</sup>  $\delta(A,B)$  between the lone-pair monosynaptic basins of the bound atoms A and B, which can be related to the number of electrons delocalized between both basins. Actually, high values (ca. 0.5) of these indexes have been found for 2c–3e bonds,<sup>74</sup> and an almost linear dependence between  $\delta(A,B)$  and the dissociation energy of the bonds has been established.<sup>75</sup> For HSeSeH, CH<sub>3</sub>SeSeCH<sub>3</sub>, and CH<sub>3</sub>SeSeNH<sub>2</sub>, the increase of the  $\delta(\text{Se},\text{Se})$  index upon electron attachment (see Table 8) indicates that this charge fluctuation is more important for the anions. Hence, a higher contribution of the ionic resonant forms Se–Se<sup>-</sup> ↔ Se–Se of the bond versus the covalent component Se<sup>.</sup>:Se should be expected, which is coherent with the disappearance of the disynaptic basin V(Se,Se) in the anions.

**Table 6.** Adiabatic EA (in eV) of the Fragments, Their Difference (in absolute value), and the Dissociation Energy (in kJ mol<sup>-1</sup>) of the Anion of the Molecule Formed by These Fragments Calculated at the CCSD(T)/aug-cc-pVTZ Level of Theory

fragment 1	EA	fragment 2	EA	$\Delta$ EA	$D_e$
HSe	1.43	HSe	1.43	0.00	104
CH <sub>3</sub> Se	1.84	CH <sub>3</sub> Se	1.84	0.00	122
CH <sub>3</sub> Se	1.84	NH <sub>2</sub> Se	1.43	0.41	92
CH <sub>3</sub> Se	1.84	OHSe	1.78	0.07	126 <sup>a</sup>
CH <sub>3</sub> Se	1.84	FSe	2.34	0.49	128 <sup>b</sup>
CH <sub>3</sub> SeSe	1.91	OH	1.74	0.17	137 <sup>c</sup>
CH <sub>3</sub> SeSe	1.91	F	3.31	1.40	77 <sup>c</sup>
OHSeSe	1.94	F	3.31	1.37	140
FSeSe	2.25	F	3.31	1.06	171
OHSe	1.78	FSe	2.34	0.56	156

<sup>a</sup> Value of the *book* isomer. <sup>b</sup> Value of the *stretched* isomer.

<sup>c</sup> Value of the *bent* isomer.

For the CH<sub>3</sub>SeSeOH *book* anion, the dissociation energy is greater than for CH<sub>3</sub>SeSeNH<sub>2</sub> coherently with the lower value of  $\Delta$ EA. For the CH<sub>3</sub>SeSeOH *stretched* isomer, the V(Se,Se) disynaptic basin disappears, because, as indicated above, in this structure the extra electron roams between the  $\sigma^*(\text{Se}–\text{Se})$  and  $\sigma^*(\text{Se}–\text{O})$  orbitals due to the comparable electronegativity of the fragments CH<sub>3</sub>Se, SeOH, CH<sub>3</sub>SeSe, and OH.  $\Delta$ EA is particularly small between the CH<sub>3</sub>Se and SeOH fragments, which explains why the spin density (Table S4 of the Supporting Information) at Se1 is higher than at O. This is also consistent with the large value of  $\delta(\text{Se},\text{Se})$  and the consequent disappearance of the disynaptic V(Se,Se) basin. The picture of the bonding is quite different, however, for the *stretched* and *bent* isomers when X = F. Due to the high EA value of F, the extra electron is close to it, and therefore the Se–Se linkage has a low 2c–3e bond character and retains a large fraction of the covalent nature which it had in the neutral. This explains the very small decrease of

**Table 7.** NBO Charge Population Analysis (in e) of the Different Radical-Anionic Structures Calculated with the BH&HLYP/6-31+G(d,p) Density<sup>a</sup>

		CH <sub>3</sub>	Se1	Se2	XH <sub>n</sub>
HSeSeH	neutral		-0.06	0.06	
	anion		-0.52	0.02	
CH <sub>3</sub> SeSeCH <sub>3</sub>	neutral		0.13	-0.13	
	anion		-0.27	-0.23	
CH <sub>3</sub> SeNH <sub>2</sub>	neutral	-0.13	0.09	0.35	-0.31
	anion	-0.23	-0.33	-0.05	-0.36
CH <sub>3</sub> SeSeOH	neutral	-0.12	0.12	0.44	-0.45
	stretched	-0.21	-0.18	-0.02	-0.58
	bent	-0.16	0.02	-0.29	-0.55
	book	-0.21	-0.30	0.02	-0.50
CH <sub>3</sub> SeSeF	neutral	-0.11	0.16	0.52	-0.57
	stretched	-0.20	-0.11	0.06	-0.74
OHSeSeF	bent	-0.15	0.04	-0.11	-0.77
	neutral	-0.43	0.52	0.47	-0.56
FSeSeF	anion	-0.49	0.02	0.23	-0.76
	neutral		0.56	-0.56	
	anion		0.19	-0.69	

<sup>a</sup> Se1 is attached to the methyl group, whereas Se2 is linked to XH<sub>n</sub>.

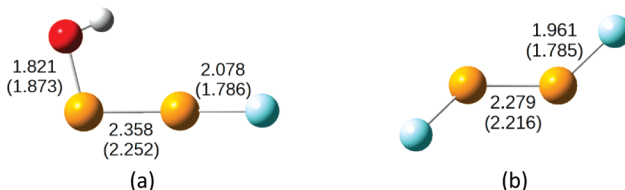
**Table 8.** Delocalization Indexes between the Lone-Pair Monosynaptic Basins of Both Selenium Atoms,  $\delta(\text{Se},\text{Se})$ , and Selenium and the Substituent X,  $\delta(\text{Se},\text{X})$ 

		$\delta(\text{Se},\text{Se})$	$\delta(\text{Se},\text{X})$
HSeSeH	neutral	0.40	
	anion	0.52	
CH <sub>3</sub> SeSeCH <sub>3</sub>	neutral	0.40	
	anion	0.57	
CH <sub>3</sub> SeSeNH <sub>2</sub>	neutral	0.21	
	anion	0.55	
CH <sub>3</sub> SeSeOH	neutral	0.45	0.53
	stretched	0.96	0.52
	bent	0.60	0.40
	book	0.59	0.57
CH <sub>3</sub> SeSeF	neutral	0.48	0.67
	stretched	0.48	0.58
	bent	0.50	0.32
OHSeSeF	neutral	0.54	0.67
	anion	0.78	0.54
FSeSeF	neutral	0.58	0.66
	anion	1.54	0.64

the electronic density at the Se—Se BCP, the negative energy density value, and the presence of a disynaptic V(Se,Se) basin.

**The Se—X Bond.** As far as the Se—O bond is concerned, the similar electron affinities of the CH<sub>3</sub>SeSe and OH fragments (see Table 6) suggest that they are prone to form 2c—3e bonds, which agrees with the high value of  $D_e$  for the *bent* anion. Actually, for both *bent* and *stretched* anions of the CH<sub>3</sub>SeSeOH system, the negative charge is evenly distributed between the CH<sub>3</sub>SeSe and OH fragments, which suggests that the charge fluctuation stabilization is high, in accordance with the high  $\delta(\text{Se},\text{O})$  index for these species.

For both *bent* and *stretched* CH<sub>3</sub>SeSeF anions, as well as for the neutral compound, there is no disynaptic V(Se,F) basin (see Figure S1 of the Supporting Information). In this respect, it is noteworthy that for FOOF an unusually long F—O distance was reported and explained in terms of an anomeric effect<sup>81</sup>—delocalization of the lone pairs of fluorine into the  $\sigma^*(\text{O}-\text{F})$  orbital. This charge delocalization would stabilize the

**Figure 6.** Main bond lengths (in Å) for the anionic derivatives of (a) OHSeSeF and (b) FSeSeF calculated at the CCSD/6-31++G(d,p) level. Values in parentheses correspond to the neutral systems.

$\sigma^*(\text{O}-\text{F})$  MO to some extent, weakening the O—F linkages and provoking this long bond distance. In our case, a similar effect could explain the absence of the disynaptic V(Se,F) basin in the neutral CH<sub>3</sub>SeSeF, which is in accordance with the high delocalization index  $\delta(\text{Se},\text{F})$ , larger than the  $\delta(\text{Se},\text{Se})$  one, and pointing out a significant charge fluctuation stabilization. The large  $\Delta E_A$  between CH<sub>3</sub>SeSe and F indicates, however, that the formation of 2c—3e bonds is not so favorable. This is clearly seen in the *bent* isomer, whose dissociation energy (77 kJ mol<sup>-1</sup>) is close to the lower bound for the dissociation limit of 2c—3e linkages (65–85 kJ mol<sup>-1</sup>). Actually, the negative charge is mainly located at the fluorine atom, and the stabilizing charge fluctuation between the V(Se) and V(F) basins decreases significantly. This limit situation is somewhat alleviated in the *stretched* isomer, where some of the extra charge goes to the Se—Se linkage (see Table 7), because the electron affinities of the fragments CH<sub>3</sub>Se and SeF are not so different. This enhances the charge fluctuation among both Se and F atoms and stabilizes the system. However, since a large fraction of the anionic charge is still at the fluorine, the charge fluctuation between both selenium atoms is not so large, and the V(Se,Se) basin is preserved.

## The Effect of Symmetry

At this point, it is worth wondering if the geometrical changes described so far are simply due to the increasing electronegativity of the substituents or whether asymmetry is also a factor to take into account. To answer this question, the molecules FSeSeOH and FSeSeF have been included in our survey. Like for CH<sub>3</sub>SeSeOH and CH<sub>3</sub>SeSeF, a *stretched* and a *bent* anion were found. However, due to the large F—Se bond length and the high acidity of the OH group, the *bent* FSeSeOH anion directly dissociates into OSeSe<sup>-</sup> + HF through a hydrogen transfer from the OH to the F arom. The *bent* anion of FSeSeF corresponds to a transition state, which lowers its energy by opening the FSeSeF dihedral angle, leading to the *stretched* isomer. Regarding the *stretched* derivatives, Figure 6 shows that the electron attachment process in both systems produces only a significant elongation of the Se—F linkage, whereas the Se—Se and the Se—O bonds remain practically unperturbed. In addition, the topology of the ELF shows no disynaptic V(Se,F) basin either in the anion or in the neutral as it occurred for CH<sub>3</sub>SeSeF (Figure 7). Interestingly, upon electron capture, the delocalization index between the selenium lone pairs increases by a factor of 3 in FSeSeF,

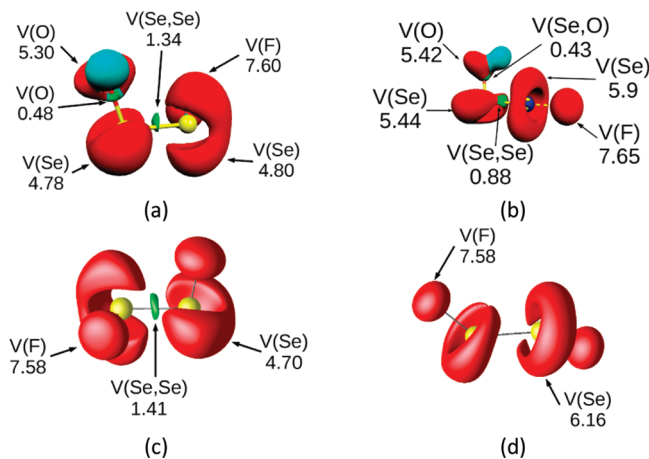


**Figure 7.** ELF localization domains within the isosurface ELF = 0.8 for the (a) neutral and (b) anionic derivatives of FSeSeOH and the (c) neutral and (d) anionic structures of FSeSeF. The same color convention as in Figure 5 is used. The population of the different basins is given in e.

the disynaptic V(Se,Se) basin disappears, and the population of the V(F) basin does not change. The natural charge of the F atoms is already  $-0.5$  in the neutral FSeSeF derivative; hence an accumulation of the extra charge on the F atoms of the anion ( $\text{Se}^{+0.5}\text{F}^{-1.0}$ ) would be highly unlikely, and only the population of the V(Se) basins increases. Obviously, both F atoms bear the same negative charge ( $-\text{FSeSeF}^{-0.5}$ ), a picture which is coherent with a significant participation of the  $\text{FSeSeF}^- \leftrightarrow \text{FSeSeF}$  resonance. As a matter of fact, the natural resonance theory shows that the resonant forms  $\text{FSeSeF}^-$  and  $\text{FSeSeF}$  contribute 53% to the total wave function. This is also consistent with a significant charge fluctuation along the Se–Se bond, which is behind the large  $\delta(\text{Se},\text{Se})$  for the anion and the disappearance of the disynaptic V(Se,Se) basin. This high charge fluctuation along the diselenide bond is less apparent in OHSeSeF since its lack of symmetry makes it possible to localize the negative charge preferentially at the fluorine atom. However, since the OH and SeSeF fragments have rather similar electron affinities, the disynaptic V(Se,Se) basin survives upon electron capture, and the Se–F linkage keeps a 2c–3e nature due to the counterbalancing effect of the OH fragment, in agreement with the high value of  $\delta(\text{Se},\text{F})$ . In conclusion, the OHSeSeF and FSeSeF systems show that, although the bond activation triggered by electron capture depends mainly on the electronegativity of the substituent X, asymmetry turns out to be a fundamental requirement to keep the covalent nature of the Se–Se linkage.

In general, the activated Se–Se and Se–X present the same topological features: the  $\nabla^2\rho$  at the BCP is near zero or large and positive, and the ELF shows no disynaptic basin in the bonding region but a large charge fluctuation between the lone-pair basins of the bonding atoms. The positive value of  $\nabla^2\rho$  as well as the absence of a disynaptic basin are typical of closed-shell interactions, but these bonds are strengthened through a charge fluctuation mechanism resulting in high  $D_e$  values. These topological features are also the signatures of the so-called *charge-shift (CS) bonds*, a new type of chemical bond proposed by Shaik and co-workers,<sup>76–78</sup> the

only difference being that CS bonds do present a disynaptic V(A,B) basin, although with a low population. In these linkages, two centers bind together not by sharing an electronic pair but by a charge fluctuation between them, exactly the same mechanism which stabilizes 2c–3e bonds. Therefore, these two types of bonds seem to be closely related, as previously suggested.<sup>74,82</sup>

## Conclusions

Through two different and complementary techniques, AIM and ELF, we have analyzed the changes of the bonding situation of a series of diselenide compounds upon electron attachment. These results have been complemented with a population analysis to locate the excess of negative charge, and the different electron affinity of the bonding fragments to rationalize their charge distribution. We have shown that, when the diselenides bear low electronegative substituents, the Se–Se bond becomes activated upon electron capture, as previous studies have shown. However, this is no longer the case for very electronegative substituents, where this bond is practically unaltered and the Se–X one is the one which elongates since the extra electron occupies the  $\sigma^*(\text{Se}-\text{X})$  antibonding orbital rather than the  $\sigma^*(\text{Se}-\text{Se})$ . When this is the case, several anionic species are also encountered, although based on the relative energies of these isomers, only one of them, namely *stretched*, should be experimentally expected. The present findings are similar to those obtained for a series of analogous disulfide derivatives, which points out that these results are not unique and could be extrapolated to a wider range of compounds than the ones covered here.

The Se–Se (and Se–X in many occasions) linkage bears some of the characteristics of the so-called charge-shift bonds, with a clear charge fluctuation between both selenium atoms. This is more evident in their anions where the bonding reflects the important contribution of the ionic resonant forms  $\text{Se}-\text{Se}^- \leftrightarrow \text{Se}-\text{Se}$  vs the covalent component  $\text{Se}:\text{Se}$ . This resonance changes with the nature of the substituents but also depends on the asymmetry of the substitution.

**Acknowledgment.** This work has been partially supported by DGI Project No CTQ2006-08558/BQU, Project MADRISOLAR2, ref.:P2009/PPQ-1533 of the Comunidad Autónoma de Madrid and by the COST Action COST CM0702. A generous allocation of computing time at the CCC of the UAM is also acknowledged. J.A.G. acknowledges a contract from the Comunidad Autónoma de Madrid.

**Supporting Information Available:** Geometries (in Cartesian coordinates) of all the compounds present in this work calculated at the CCSD/6-31++G(d,p) level of theory, charge analysis and the corresponding discussion to assess the reliability of the MP2 approach, HF eigenvalues of the SOMOs of the most stable anionic species, NBO spin densities of all the anions, and the ELF analysis of all the neutral molecules. This material is available free of charge via the Internet at <http://pubs.acs.org>.

## References

- (1) Schwarz, K.; Foltz, C. M. *J. Am. Chem. Soc.* **1957**, *79*, 632.
- (2) Shchedrina, V. A.; Novoselov, S. V. *Proc. Natl. Acad. Sci. U.S.A.* **2007**, *104*, 13919.
- (3) Kryukov, G. V.; Castellano, S.; Novoselov, S. V.; Lobanov, A. V.; Zehtab, O.; Guigo, R.; Gladyshev, V. N. *Science* **2003**, *300*, 1439.
- (4) Behne, D. Pfeifer, H. Rothlein, D. Kyriakopoulos, A. *Proceedings of the 10th International Symposium on Trace Elements in Man and Animals*; Plenum Press: New York, 2000.
- (5) Castellano, S.; Lobanov, A. V.; Chapple, C.; Novoselov, S. V.; Albercht, M.; Hua, D.; Lesc7ure, A.; Lengauer, T.; Krol, A.; Gladyshev, V. N.; Guigo, R. *Proc. Natl. Acad. Sci. U.S.A.* **2005**, *102*, 16188.
- (6) Rayman, M. P. *Lancet* **2000**, *356*, 233.
- (7) Chen, J.; Berry, M. J. *J. Neurochem.* **2003**, *86*, 1.
- (8) Schomburg, L.; Schweizer, U.; Koehrle, J. *Cell. Mol. Life Sci.* **2004**, *61*, 1988.
- (9) Frank, W. Z. *Physiol. Chem.* **1964**, *339*, 222.
- (10) Walter, R.; du Vigneaud, V. *J. Am. Chem. Soc.* **1965**, *87*, 4192.
- (11) Walter, R.; du Vigneaud, V. *J. Am. Chem. Soc.* **1966**, *88*, 1331.
- (12) Hartrodt, B.; Neubert, K.; Bierwolf, B.; Blech, W.; Jakubke, H. D. *Tetrahedron Lett.* **1980**, *21*, 2393.
- (13) Besse, D.; Budisa, N.; Karnbrock, W.; Minks, C.; Musiol, H. J.; Pegararo, S.; Siedler, F.; Weyher, E.; Moroder, L. *J. Biol. Chem.* **1997**, *378*, 211.
- (14) Koider, T.; Itoh, H.; Otaka, A.; Furuya, M.; Kitajima, Y.; Fujii, N. *Chem. Pharm. Bull.* **1993**, *46*, 5382.
- (15) Rajarathnam, K.; Sykes, B. D.; Dewald, B.; Baggioolini, M.; Clark-Lewis, I. *Biochemistry* **1999**, *38*, 7653.
- (16) Metanis, N.; Keinan, E.; Dawson, P. E. *J. Am. Chem. Soc.* **2006**, *128*, 16684.
- (17) Armishaw, C. J.; Daly, N. T.; Adams, D. J.; Craik, D. J.; Alewook, P. F. *J. Biol. Chem.* **2006**, *281*, 14136.
- (18) Fori, S.; Pegararo, S.; Rudolph-Böhner, S.; Cramer, J.; Moroder, L. *Biopolymers* **2000**, *53*, 550.
- (19) Hondal, R. J.; Nilsson, B. L.; Raines, R. T. *J. Am. Chem. Soc.* **2001**, *123*, 5140.
- (20) Nutt, R. F.; Veber, D. F.; Saperstein, R. *J. Am. Chem. Soc.* **1980**, *102*, 6539.
- (21) Stymiest, J. L.; Mitchell, B. F.; Wong, S.; Vederas, J. C. *Org. Lett.* **2003**, *5*, 47.
- (22) Hargittai, B.; Sole, N. A.; Groebe, D. R.; Abramson, S. N.; Barany, G. *Med. Chem.* **2000**, *43*, 4787.
- (23) Bondebjerg, J.; Grunnet, M.; Jespersen, T.; Meldal, M. *Chem. Biol. Chem.* **2003**, *4*, 186.
- (24) Jacob, C.; Giles, G. I.; Giles, N. M.; Sies, H. *Angew. Chem., Int. Ed.* **2003**, *42*, 4742.
- (25) Johansson, I.; Gafvelin, G.; Amér, E. S. *Biochim. Biophys. Acta* **2005**, *1726*, 1.
- (26) Sheu, C.; Sobkowiak, A.; Zhang, L.; Ozbalik, N.; Barton, D. H. R.; Sawyer, D. T. *J. Am. Chem. Soc.* **1989**, *111*, 8030.
- (27) Tian, F.; Yu, Z.; Lu, S. *J. Org. Chem.* **2004**, *69*, 4520.
- (28) Degrand, C.; Nour, M. *J. Electroanal. Chem.* **1984**, *190*, 213.
- (29) Barbosa, N. B. V.; Rocha, J. B. T.; Wondracek, D. C.; Petroni, J.; Zeni, G.; Nogueira, C. W. *Chem. Biol. Interact.* **2006**, *3*, 230.
- (30) de Freitas, A. S.; Funck, V. R.; Rotta, M. d. S.; Bohrer, D.; Mörschbächer, V.; Puntel, R. L.; Nogueira, C. W.; Farina, M.; Aschner, M.; Rocha, J. B. T. *Brain Res. Bull.* **2009**, *79*, 77–84.
- (31) Arteel, G. E.; Sies, H. *Environ. Toxicol. Pharmacol.* **2001**, *10*, 153.
- (32) Meotti, F. C.; Stangerlin, E. C.; Zeni, G.; Nogueira, C. W.; Rocha, J. B. T. *Environ. Res.* **2004**, *94*, 276.
- (33) Kumar, B. S.; Kunwar, A.; Ahmad, A.; Kumbhare, L. B.; Jain, V. K.; Priyadarsini, K. I. *Radiat. Environ. Biophys.* **2009**, *48*, 379.
- (34) Pearson, J. K.; Boyd, R. J. *J. Phys. Chem. A* **2007**, *111*, 3152–3160.
- (35) Antonello, S.; Daasbjerg, K.; Jensen, H.; Taddei, F.; Maran, F. *J. Am. Chem. Soc.* **2003**, *125*, 14905–14916.
- (36) Sobczyk, M.; Simons, J. *Int. J. Mass Spectrom.* **2006**, *253*, 274–280.
- (37) Anusiewicz, I.; Berdys-Kochanska, J.; Simons, J. *J. Phys. Chem. A* **2005**, *109*, 5801–5813.
- (38) Modelli, A.; Jones, D. *J. Phys. Chem. A* **2006**, *110*, 13195–13201.
- (39) Yamaji, M.; Tojo, S.; Takehira, K.; Tobita, S.; Fujitsuka, M.; Majima, T. *J. Phys. Chem. A* **2006**, *110*, 13487–13491.
- (40) Meija, J.; Beck, T. L.; Caruso, J. A. *J. Am. Soc. Mass Spectrom.* **2004**, *15*, 1325–1332.
- (41) Modelli, A.; Jones, D.; Distefano, G.; Tronc, M. *Chem. Phys. Lett.* **1991**, *181*, 361.
- (42) Gámez, J. A.; Serrano-Andrés, L.; Yáñez, M. *Phys. Chem. Chem. Phys.* **2010**, *5*, 1042.
- (43) Gräfenstein, J.; Kraka, E.; Cremer, D. *J. Chem. Phys.* **2004**, *120*, 528–538.
- (44) Polo, V.; Gräfenstein, J.; Kraka, E.; Cremer, D. *Chem. Phys. Lett.* **2002**, *352*, 469–478.
- (45) Gräfenstein, J.; Kraka, E.; Cremer, D. *Phys. Chem. Chem. Phys.* **2004**, *6*, 1096–1112.
- (46) Cohen, A.; Mori-Sánchez, P.; Yang, W. *Science* **2008**, *321*, 792–794.
- (47) Curtiss, L. A.; Redfren, P. C.; Raghavachari, K.; Pople, J. A. *J. Chem. Phys.* **1998**, *109*, 42.
- (48) Rienstra-Kiracofe, J. C.; Tschumper, G. S.; Schaefer, H. F., III; Nandi, S.; Ellison, G. B. *Chem. Rev.* **2002**, *102*, 231–282.
- (49) van Doren, J. M.; Miller, T. M.; Viggiano, V. V. *J. Chem. Phys.* **2008**, *128*, 094310–094317.
- (50) Braïda, B.; Hiberty, P. C.; Savin, A. *J. Phys. Chem. A* **1998**, *102*, 7872–7877.
- (51) Becke, A. D. *J. Chem. Phys.* **1993**, *98*, 1372.
- (52) Lee, C.; Yang, W.; Parr, R. G. *J. Phys. Rev. B* **1988**, *37*, 785.
- (53) Braïda, B.; Hiberty, P. C. *J. Phys. Chem. A* **2000**, *104*, 4618.
- (54) Braïda, B.; Hiberty, P. C. *J. Phys. Chem. A* **2003**, *107*, 4741.

- (55) Kaur, D.; Sharma, P.; Bharatam, P. V. *THEOCHEM* **2007**, *810*, 31–37.
- (56) Frisch, M. J.; Trucks, G. W.; Schlegel, H. B.; Scuseria, G. E.; Robb, M. A.; Cheeseman, J. R.; Montgomery, J. A., Jr.; Vreven, T.; Kudin, K. N.; Burant, J. C.; Millam, J. M.; Iyengar, S. S.; Tomasi, J.; Barone, V.; Mennucci, B.; Cossi, M.; Scalmani, G.; Rega, N.; Petersson, G. A.; Nakatsuji, H.; Hada, M.; Ehara, M.; Toyota, K.; Fukuda, R.; Hasegawa, J.; Ishida, M.; Nakajima, T.; Honda, Y.; Kitao, O.; Nakai, H.; Klene, M.; Li, X.; Knox, J. E.; Hratchian, H. P.; Cross, J. B.; Bakken, V.; Adamo, C.; Jaramillo, J.; Gomperts, R.; Stratmann, R. E.; Yazyev, O.; Austin, A. J.; Cammi, R.; Pomelli, C.; Ochterski, J. W.; Ayala, P. Y.; Morokuma, K.; Voth, G. A.; Salvador, P.; Dannenberg, J. J.; Zakrzewski, V. G.; Dapprich, S.; Daniels, A. D.; Strain, M. C.; Farkas, O.; Malick, D. K.; Rabuck, A. D.; Raghavachari, K.; Foresman, J. B.; Ortiz, J. V.; Cui, Q.; Baboul, A. G.; Clifford, S.; Cioslowski, J.; Stefanov, B. B.; Liu, G.; Liashenko, A.; Piskorz, P.; Komaromi, I.; Martin, R. L.; Fox, D. J.; Keith, T.; Al-Laham, M. A.; Peng, C. Y.; Nanayakkara, A.; Challacombe, M.; Gill, P. M. W.; Johnson, B.; Chen, W.; Wong, M. W.; Gonzalez, C.; Pople, J. A. *Gaussian 03*; Gaussian Inc.: Wallingford, CT, 2004.
- (57) Werner, H.-J.; Knowles, P. J.; Lindh, R.; Manby, F. R.; Schütz, M.; Celani, P.; Korona, T.; Mitrushenkov, A.; Rauhut, G.; Adler, T. B.; Amos, R. D.; Bernhardsson, A.; Berning, A.; Cooper, D. L.; Deegan, M. J. O.; Dobbyn, A. J.; Eckert, F.; Goll, E.; Hampel, C.; Hetzer, G.; Hrenar, T.; Knizia, G.; Köppel, C.; Liu, Y.; Lloyd, A. W.; Mata, R. A.; May, A. J.; McNicholas, S. J.; Meyer, W.; Mura, M. E.; Nicklass, A.; Palmieri, P.; Pflüger, K.; Pitzer, R.; Reiher, M.; Schumann, U.; Stoll, H.; Stone, A. J.; Tarroni, R.; Thorsteinsson, T.; Wang, M.; Wolf, A. *MOLPRO 2009.01*; Cardiff University: Cardiff, U. K., 2009.
- (58) Pierloot, K.; Dumez, B.; Widmark, P.-O.; Roos, B. O. *Theor. Chem. Acta* **1995**, *90*, 87.
- (59) Veryazov, V.; Widmark, P.-O.; Serrano-Andrés, L.; Lindh, R.; Roos, B. O. *Int. J. Quantum Chem.* **2004**, *100*, 626–635.
- (60) Matta, C. F.; Boyd, R. J. In *The Quantum Theory of Atoms in Molecules*; Matta, C. F., Boyd, R. J., Eds.; Wiley: Weinheim, Germany, 2007; pp 1–30.
- (61) Kohout, M. *DGrid*, version 4.5; Federal Ministry of Education and Research: Radebeul, Germany, 2009.
- (62) Becke, A. D.; Edgecombe, K. E. *J. Chem. Phys.* **1990**, *92*, 5397.
- (63) Silvi, B.; Savin, A. *Nature* **1994**, *371*, 683.
- (64) Silvi, B. *Phys. Chem. Chem. Phys.* **2004**, *6*, 256.
- (65) Noury, S.; Krokidis, X.; Fuster, F.; Silvi, B. *Comput. Chem.* **1999**, *23*, 597.
- (66) Groner, P.; Gillies, C. W.; Gillies, J. Z.; Zhang, Y.; Block, E. *J. Mol. Spectrosc.* **2004**, *226*, 169–181.
- (67) Carles, S.; Lecomte, F.; Schermann, J. P.; Desfrancois, C.; Xu, S.; Nilles, J. M.; Bowen, K. H.; Berges, J.; Houee-Levin, C. *J. Phys. Chem. A* **2001**, *105*, 5622–5626.
- (68) Pauling, L. *J. Am. Chem. Soc.* **1931**, *53*, 3225–3237.
- (69) Pauling, L. *J. Chem. Phys.* **1933**, *1*, 56–59.
- (70) Hiberty, P. C.; Humbel, S.; Archirel, P. *J. Phys. Chem.* **1994**, *98*, 11697–11704.
- (71) Hiberty, P. C.; Shaik, S. In *Valence Bond Theory*; 1st ed.; Cooper, D. L., Ed.; Elsevier: Amsterdam, 2002; pp 207–214.
- (72) Clark, T. *J. Am. Chem. Soc.* **1988**, *110*, 1672–1678.
- (73) Fradera, X.; Auster, M. A.; Bader, R. F. W. *J. Phys. Chem. A* **1999**, *103*, 304.
- (74) Fourré, I.; Silvi, B. *Heteroatom Chem.* **2007**, *18*, 135.
- (75) Fourré, I.; Silvi, B.; Sevin, A.; Chevreau, H. *J. Phys. Chem. A* **2002**, *106*, 2651–2571.
- (76) Shaik, S.; Danovich, D.; Silvi, B.; Lauvergnat, D.; Hiberty, P. *Chem.—Eur. J.* **2005**, *11*, 6358.
- (77) Zhang, L.; Ying, F.; Wu, W.; Hiberty, P.; Shaik, S. *Chem.—Eur. J.* **2009**, *15*, 2979.
- (78) Wu, W.; Song, J.; Shaik, S.; Hiberty, P. *Angew. Chem., Int. Ed.* **2009**, *48*, 1407.
- (79) Hiberty, P. C.; Humbel, S.; Archirel, P. *J. Phys. Chem. A* **1994**, *98*, 11697.
- (80) Fourré, I.; Bergès, J. *J. Phys. Chem. A* **2004**, *108*, 898–906.
- (81) Kraka, E.; He, Y.; Cremer, D. *J. Phys. Chem. A* **2001**, *105*, 3269–3276.
- (82) Bil, A.; Berski, S.; Latajka, Z. *J. Chem. Inf. Model.* **2007**, *47*, 1021–1030.

CT100336Q